IEEE Access
Multidisciplinary | Rapid Review | Open Access Journal

Received November 28, 2019, accepted December 31, 2019, date of publication January 6, 2020, date of current version January 21, 2020.

Digital Object Identifier 10.1109/ACCESS.2020.2963852

Data-Driven Analysis of Traffic Volume and Hub City Evolution of Cities in the Guangdong-Hong Kong-Macao Greater Bay Area

PEIQUN LIN[1], YITAO HE[1], AND MINGYANG PEI[1,2]
[1]Department of Civil and Transportation Engineering, South China University of Technology, Guangzhou 510641, China
[2]Department of Civil and Environmental Engineering, University of South Florida, Tampa, FL 33620, USA

Corresponding author: Mingyang Pei (ratherthan@foxmail.com)

This work was supported in part by the National Natural Science Foundation of China under Grant U1811463, in part by the Science and Technology Program Project of Guangdong Province under Grant 2017B030307001 and Grant 2016A040403045, and in part by the Science and Technology Program Project Grant of Guangzhou under Grant 201807010008 and Grant 201803030045.

ABSTRACT The longest cross-sea bridge worldwide, i.e., the Hong Kong-Zhuhai-Macao Bridge (HZMB), opened in October 2018, integrating nine cities and two special administrative regions of China's Guangdong-Hong Kong-Macao Greater Bay Area (GBA). The GBA is one of the regions with the most active economic vitality in China and has an important strategic position in the overall national development. Using full-sample freeway toll data of the GBA, this paper proposed a new structured evaluation methodology that combines the node degree, traffic volume, and topological and flow field-theory (e.g., agglomeration and distribution) to explore the hub city ranking and evolution in this area. The data period we selected to analyze is immediately before and after the opening of the HZMB, and we assess the counties' centrality changes in the GBA by analyzing these data. The findings reported in this paper can reflect the traffic hub evaluation process and provide more macroscopic intercity transportation views to the government.

INDEX TERMS Data analysis, Guangdong-Hong Kong-Macao greater bay area (GBA), Hong Kong-Zhuhai-Macao bridge (HZMB), hub city evolution.

I. INTRODUCTION

China's Guangdong-Hong Kong-Macao Greater Bay Area (GBA) covers a total area of 56,000 square kilometers and links Hong Kong, Macao, Guangzhou, Shenzhen and seven other cities with a combined population of 70 million [1]; the objective of the GBA is to become the fourth largest bay area worldwide and build a world-class urban agglomeration [2]–[4]. The other three largest bay areas, including the Tokyo Bay Area, New York Bay Area, and San Francisco Bay Area, benefit from their highly connected freeways and bridges. The Golden Gate Bridge, which is located on the Golden Gate Strait in San Francisco, is not only a landmark architecture but also a significant corridor in the San Francisco Bay Area [5]. The Bronx-Whitestone Bridge and Tokyo Bay Bridge also play significant roles in connecting traffic on both sides of the bay area [6]. TABLE 1 shows a comparison of four major bay areas in terms of the field of zone space, population, GDP, and vital infrastructures.

As shown in TABLE 1, the Hong Kong-Zhuhai-Macao Bridge (HZMB) is considered the most vital infrastructure of the GBA that increases the spatial disparity of accessibility [20] and plays an essential role in promoting transportation connectivity and economic integration [21]. FIGURE 1 shows the geographic locations of the GBA, HZMB, and data collection points in this paper. The GBA is a sharp heart space with the largest cities in the central area [1]. Thus, the HZMB is located in an essential geographic location in the GBA.

The HZMB, which opened to traffic in October 2018, strengthens the transport links between the Mainland and Hong Kong and Macao [18], [19] and builds an efficient and convenient modern integrated transport system. The HZMB is designed to have a traffic capacity of $2.5 * 10^6$ per

The associate editor coordinating the review of this manuscript and approving it for publication was Chintan Amrit.

TABLE 1. Comparison of the four largest bay areas.

Urban agglomeration	Country	Area of zone /10^5 km^2	Population /million	GDP/$	Vital infrastructure
New York Bay Area [6]-[8]	U.S.	0.22	2.34	$1.4*10^{12}$	Long Island Expressway Bronx-Whitestone Bridge I-678 N
San Francisco Bay Area [5], [9]-[11]	U.S.	0.18	0.76	$0.8*10^{12}$	Golden Gate Bridge CA–92 W San Francisco-Oakland Bay Bridge
Tokyo Bay Area [12, 13]	Japan	0.37	4.35	$1.8*10^{12}$	Tokyo Bay Bridge Tokyo Bay Expressway
GBA [14]-[17]	China	0.56	6.67	$1.36*10^{12}$	Hong Kong-Zhuhai-Macao Bridge (HZMB) Humen Bridge Pearl River Delta Ring Freeway

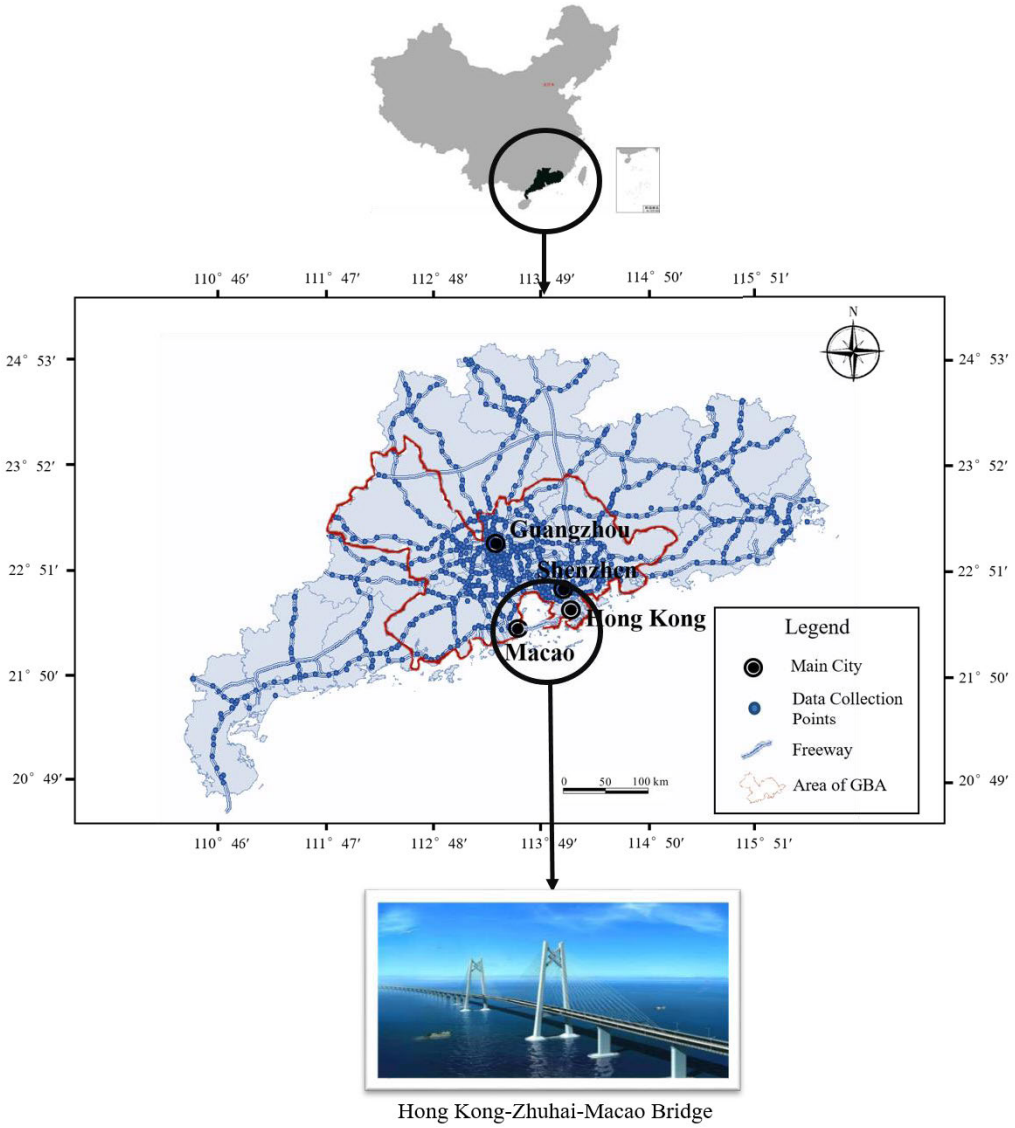

FIGURE 1. Geographic locations of the GBA, HZMB, and data collection points in this paper.

month [22]. Since the vehicle quota policy has not been fully liberalized on this newly constructed bridge, the traffic volume is only $1.4*10^5$ per month on average by July 2019 (data from the Transport Department of the Hong Kong Special Administrative Region). As shown in FIGURE 2, the total vehicle volume on the HZMB is steadily increasing.

Since the GBA is one of the most competitive urban agglomerations worldwide, studying the traffic

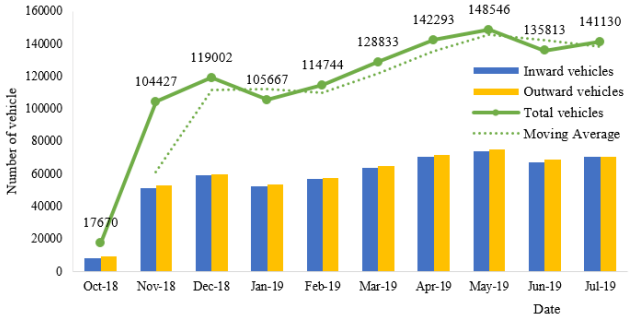

FIGURE 2. Total vehicle volume on the HZMB on the HK side (month).

characteristics of urban agglomeration and city ranking can help explore the transportation evolution mode and provide data supporting future research in this area. Thus, we need to select some traffic evaluation indexes, e.g., node degree, traffic volume, agglomeration, and distribution characteristic indexes. Significant studies performed over recent years have investigated the node degree, traffic volume, agglomeration, and distribution field.

The node degree can be selected as an index for node importance assessment in a transportation network [23]–[29]. In traffic networks, the node degree distribution is an essential factor in scale-free networks [30], and the node-to-node distance based on both the definition of the norm and node degree is provided to avoid traffic concentration problems [31]. By showing that the best routing metric is the ??-norm based on node degrees along a path to the destination node, Tamura H [32] addresses the issue of network congestion due to inef?cient mapping between traf?c demand and network resources. Studies investigating the relationship between the node degree and city centrality are significant for traffic design [35].

Recently, the traffic volume index has been mainly used in traffic management [36], especially in traffic prediction through long short-term memory (LSTM) and deep belief network (DBN) [37]. Wang *et al.* [38] analyzed the interactive pattern of traffic flow in three macro-regions based on real Beijing expressway toll collection data and calculated the traffic volume to determine the specific relationships of the traffic volume in these large OD regions during different periods.

Many scholars have also studied the agglomeration and distribution field to discover the pattern within a specific field. Lewin [39] first applied the theory of agglomeration and distribution in the field of social psychology. This theory is also widely applied in the transportation and tourism field. Berry [40] first applied the theory of the ''space field'' to the spatial analysis of cargo flow, and this theory supports the assessment of the potential of the development of a logistics and transport hub through the calculation of relevant indicators using available information regarding container flows in the region [41]. By analyzing agglomeration and distribution tourist fields in Europe, the geographical pattern of tourist-destination and tourist-generating areas becomes clear [42], [43].

With the expansion of city scope and the increasing number of cities, there has been a rapid development in the study of urban hierarchical patterns and spatial structures. The K-means clustering algorithm [44], Gravity Model [45], and central place theory [46] are used to analyze cities' functional structures and the hierarchy evolution of urban agglomerations. Remote sensing data and nighttime light data are also applied to explore the dynamics of polycentric urban development [47], [48]. Other data resources (i.e., population, wealth, etc.) display a positive correlation with topological and dynamic centrality [49].

Although previous studies are thorough and intensive in analyzing city centrality and spatial structures, some problems remain to be addressed. Due to the lack of long term and full sample traffic data [36], [42], most previous studies were carried out using the method of comparison [50] or theoretical analyses [51]; other studies rely on a sample of open source or macro data (e.g., such as road network structure data [29] and social and economic indicators data [44]), which may lead to one-sided and subjective results in the analysis. Additionally, the evaluation system cannot comprehensively consider more indexes (e.g., agglomeration and distribution function and urban hierarchical pattern), and the two indexes, i.e., the node degree and traffic volume, reflecting district accessibility and district centrality are not considered simultaneously.

To bridge these research gaps, this paper analyzes the traffic hub city evolution of the GBA and makes the following contributions.

First, the GBA is among the regions with the most active economic vitality in China; however, few studies have focused on hub city evaluations in this area, and full sample extensive data-driven studies are scarce. The data used in this research are collected from a total number of 610 toll stations with a total number of 1.4 million pieces of toll notes over 6 months. The data period we analyze is immediately before and after the opening of the HZMB; thus, we provide reliable and abundant benchmark data.

Second, we propose an evaluation model that combines the unit area node degree and the scores obtained from an R-mode analysis and Q-mode analysis. The conclusions obtained from the proposed evaluation model have a high application value. These data can reflect the hub city evolution trend for the government.

The remainder of this paper is organized as follows. Section 2 presents the study area of this paper. Section 3 introduces the methodology of this research, including the node degree method and agglomeration and distribution method. Section 4 provides the data preparation process and discusses the three vital indexes (i.e., node degree, traffic volume, agglomeration, and distribution). Section 4 analyzes the results of the proposed model and performs some sensitivity analyses. Section 5 offers a conclusion.

II. STUDY AREA

The research area in this study is the GBA (114°47'-114°53'E, 21°50'-23°53'N), which includes

eleven cities (i.e., Guangzhou, Shenzhen, Zhuhai, Foshan, Huizhou, Dongguan, Zhongshan, Jiangmen, Zhaoqing, Hong Kong, and Macao) and covers a total area of 56,000 square kilometers. To deeply analyze the characteristics of the hub cities in the GBA (e.g., node degree, traffic volume, agglomeration, and distribution), we divide the GBA into forty-three research-units according to the following rules:

① *Administrative Rules:* Since it is easier to obtain data by administrative region, we divide and integrate the units based on the 91 existing administrative counties.

② *Connectivity Rules:* We consider protecting the fundamental role of each unit (e.g., tight economic connection, life-oriental tour connection district, etc.) and maintain the district traffic functions' integrity. For example, since the central urban area of Guangzhou has close connections by city roads and fewer freeway connections, we integrate the area of the central counties in Guangzhou as a unit to avoid interrupting the highly integrated unit characteristic.

③ *Data Source Rules:* The data quality in some regions is slightly lower since the frequency administrative division adjustment by the government causes data duplication and missing data. Adjusting or merging some existing administrative counties can improve the data quality and accuracy of the analysis.

Proper research units are conducive for the data acquisition and cleaning processes and increase the data accuracy. The zoning results are shown in TABLE 2 and FIGURE 3.

With the increasing attention to data-driven analyses, scholars have increasingly focused on the full sample analysis of massive data and explored the patterns in such data [52]–[57]. The toll data used in this paper are derived from the Guangdong Provincial Department of Transportation and cover over 4000 kilometers of freeway mileage across all 610 data-collection points [1]. Since China's freeway network has restricted access, the toll records can accurately describe all vehicles' travel characteristics (e.g., origins and destinations, departure and arrival times, vehicle types, toll fees, etc.). As shown in Table 2 in the sixth column, the number of data points reaches 65 million per month.

Regarding the research period, we select the months immediately before and after the opening of the HZMB (i.e., 2018 and 2019) and compare regular months (e.g., January and March) to selected national festival months (e.g., February, which includes the Spring Festival, the Lantern Festival, etc.).

Regarding both geographical and economical consideration, the central area of the GBA includes counties belonging to GZ, FS, ZS, DG, SZ, ZH, HK, and MO, while the edge area of the GBA includes counties belonging to JM, HZ and ZQ [1]. To analyze the influence of the HZMB in the GBA in-depth, we marked the bankside of the HZMB in FIGURE 3. In FIGURE 3, the area in the blue circle represents the east-side cities of the HZMB (i.e., MO, XZ, ZS, DM, TS, and XH), while the red circle area represents the west side cities of the HZMB (i.e., LH, SZ, LG, BA, and HK), all of which are located within a radius of 50 km.

III. METHODOLOGY

For the convenience of the readers, the critical notations used throughout the paper are summarized in TABLE 3.

The hub city evaluation model includes the following two components: the score of the improved unit area node degree (i.e., k_i/A_i) and the scores of the agglomeration-distribution analyses (i.e., $F_{1,i}$ and $F_{2,i}$).

$$M_i = c_1 \frac{k_i}{A_i} + c_2(F_{1,i} + F_{2,i}) \quad i \in \mathcal{J} \tag{1}$$

In Equation (1), M_i denotes the score of the evaluation of district i, and c_1 and c_2 denote the coefficients of the rate of the score of the unit area node degree and the rate of the score of the R-mode and Q-mode analyses, respectively. In the first component, k_i/A_i denotes the node degree divided by the acreage of district i. In the second component, $F_{1,i}$ denotes the score of the R-mode analysis, and $F_{2,i}$ denotes the score of the Q-mode analysis. This model considers the intercity traffic connections and their traffic volume simultaneously, thus avoiding one-sided conclusions.

A. NODE DEGREE

The node degree is the number of links associated with a particular node in a network, is often proportional to the importance of the node [29] and has been regarded as one of the essential and convenient metrics used to measure the connectivity of specific networks [58],[59]. The node degree (k_i) is the sum of the out-degree ($\sum_{i\neq j, j\in\mathcal{J}} \alpha_{ij}$) and in-degree ($\sum_{i\neq j, j\in\mathcal{J}} \alpha_{ji}$). The out-degree refers to the number of links that flow in the direction from that node to other nodes, and the in-degree refers to the number of links that flow in the direction from other nodes to that node. In Equation (2), α_{ij} denotes the number of links from district i to district j, while α_{ji} denotes the number of links from district j to district i. These two vital components represent the out-degree and in degree, and their sum represents the node degree of node i.

$$k_i = \sum_{i\neq j, j\in\mathcal{J}} \alpha_{ij} + \sum_{i\neq j, j\in\mathcal{J}} \alpha_{ji} \quad \forall i \in \mathcal{J} \tag{2}$$

B. AGGLOMERATION AND DISTRIBUTION

To address the question of agglomeration and distribution, we introduce a factor analysis in our research. Factor analysis is a traditional method used to identify the socio-economic structure of urban areas [60] and has been used in a considerable number of papers [61], [62].

Factor analysis uses the data collected from the 43 research units to form a 43 × 43 R-mode original matrix $\boldsymbol{X}$ and a Q-mode matrix $\boldsymbol{X^T}$, where $\boldsymbol{X}$ and $\boldsymbol{X^T}$ are transposed-matrix. The R-mode analysis can analyze the agglomeration patterns and show the destinations' typical type, while the Q-mode analysis reveals the distribution pattern and shows the origins' typical type [60]. In the matrices $\boldsymbol{X}$ and $\boldsymbol{X^T}$, the matrix

TABLE 2. Zoning results and necessary information.

District number	District name	Abbreviation name	Affiliation city	Space/ km²	Population /million	Number of data collection stations	Total number of data records [1*]	Applicable partition rules
1	Guangzhou	GZ[2*]	Guangzhou	280	5.59	22	12.22*10⁷	①②
2	Baiyun	BY	Guangzhou	796	2.71	46	18.37*10⁷	①
3	Huangpu	HP	Guangzhou	484	1.11	17	2.10*10⁷	①
4	Panyu	PY	Guangzhou	786	1.78	22	6.83*10⁷	①
5	Nansha	NS	Guangzhou	528	0.75	23	2.69*10⁷	①
6	Zengcheng	ZC	Guangzhou	1617	1.22	24	1.94*10⁷	①
7	Huadu	HD	Guangzhou	970	1.09	25	2.90*10⁷	①
8	Conghua	CH	Guangzhou	1975	0.65	17	1.04*10⁷	①
9	Chancheng	CC	Foshan	154	1.13	3	1.41*10⁷	①②
10	Nanhai	NH	Foshan	1073	2.62	26	6.07*10⁷	①
11	Shunde	SD	Foshan	806	2.61	13	3.92*10⁷	①
12	Gaoming	GM	Foshan	960	0.48	9	0.71*10⁷	①
13	Sanshui	SS	Foshan	827	0.65	9	1.42*10⁷	①
14	Zhongshan	ZS	Zhongshan	1784	3.26	25	3.95*10⁷	①
15	Dongguan	DG	Dongguan	2465	8.39	60	18.12*10⁷	①
16	Shenzhen	SZ[2*]	Shenzhen	420	4.25	15	10.85*10⁷	①②
17	Bao'an	BA	Shenzhen	552	3.75	30	10.33*10⁷	①③
18	Longgang	LG	Shenzhen	850	2.85	35	15.39*10⁷	①③
19	Longhua	LH	Shenzhen	176	1.60	8	4.77*10⁷	①
20	Xiangzhou	XZ	Zhuhai	555	1.10	7	1.36*10⁷	①
21	Doumen	DM	Zhuhai	1181	0.79	6	2.37*10⁷	①③
22	Pengjiang	PJ	Jiangmen	320	0.76	11	1.19*10⁷	①
23	Jianghai	JH	Jiangmen	111	0.29	4	0.59*10⁷	①
24	Xinhui	XH	Jiangmen	1387	0.89	7	0.46*10⁷	①
25	Taishan	TS	Jiangmen	3285	0.97	14	0.87*10⁷	①
26	Kaiping	KP	Jiangmen	1658	0.73	5	0.51*10⁷	①
27	Enping	EP	Jiangmen	1696	0.52	4	0.27*10⁷	①
28	Heshan	HS	Jiangmen	1083	0.53	11	0.56*10⁷	①
29	Huicheng	HC	Huizhou	1501	1.29	19	2.70*10⁷	①
30	Huiyang	HY	Huizhou	915	0.65	21	2.76*10⁷	①
31	Huidong	HDO	Huizhou	3527	1.27	13	1.01*10⁷	①
32	Boluo	BL	Huizhou	2858	1.21	16	1.92*10⁷	①
33	Longmen	LM	Huizhou	2295	0.36	4	0.31*10⁷	①
34	Duanzhou	DZ	Zhaoqing	154	0.51	2	0.43*10⁷	①
35	Dinghu	DH	Zhaoqing	552	0.18	6	0.49*10⁷	①
36	Guangning	GN	Zhaoqing	2455	0.44	4	0.28*10⁷	①
37	Huaiji	HJ	Zhaoqing	3554	0.85	5	0.28*10⁷	①
38	Fengkai	FK	Zhaoqing	2723	0.42	3	0.14*10⁷	①
39	Deqing	DQ	Zhaoqing	2003	0.36	3	0.15*10⁷	①
40	Gaoyao	GY	Zhaoqing	2186	0.80	9	1.35*10⁷	①
41	Sihui	SH	Zhaoqing	1263	0.59	5	0.73*10⁷	①
42	Hong Kong	HK[3*]	Hong Kong	1106	7.48	-	0.38*10⁷	①
43	Macao	MO[3*]	Macao	33	0.66	-	0.05*10⁷	①

Note: 1*. The data period is from Jan to Mar in 2018 and 2019.
2*. GZ and SZ refer to the Guangzhou Urban district and Shenzhen Urban district, respectively.
3*. Since there are no data collection points in Hong Kong and the Macao city area, this paper uses the nearest collection points instead.

element x_{ij} denotes the traffic flow volume from the origin i to destination j, where $\forall i, j \in \mathcal{J}$.

Equations (3), (4), and (5) show the data standardization process. In these Equations, x'_{ij} denotes the revised traffic volume from district $i \in \mathcal{J}$ to $j \in \mathcal{J}$, $\bar{x}_i$ denotes the average traffic volume starting from district $i \in \mathcal{J}$, and S_i denotes the variance of the traffic volume starting from district $i \in \mathcal{J}$.

$$x'_{ij} = \frac{x_{ij} - \bar{x}_i}{S_i} \quad \forall i, j \in \mathcal{J} \tag{3}$$

$$\bar{x}_i = \frac{1}{n}\sum_{k=1}^{n} x_{ik} \quad \forall i, k \in \mathcal{J} \tag{4}$$

$$S_i = \sqrt{\frac{1}{n-1}\sum_{k=1}^{n}(x_{ik} - \bar{x}_i)^2} \quad \forall i, k \in \mathcal{J} \tag{5}$$

Then, the correlation coefficient can be calculated by Equation (6), where R_{ij} is the correlation coefficient of the

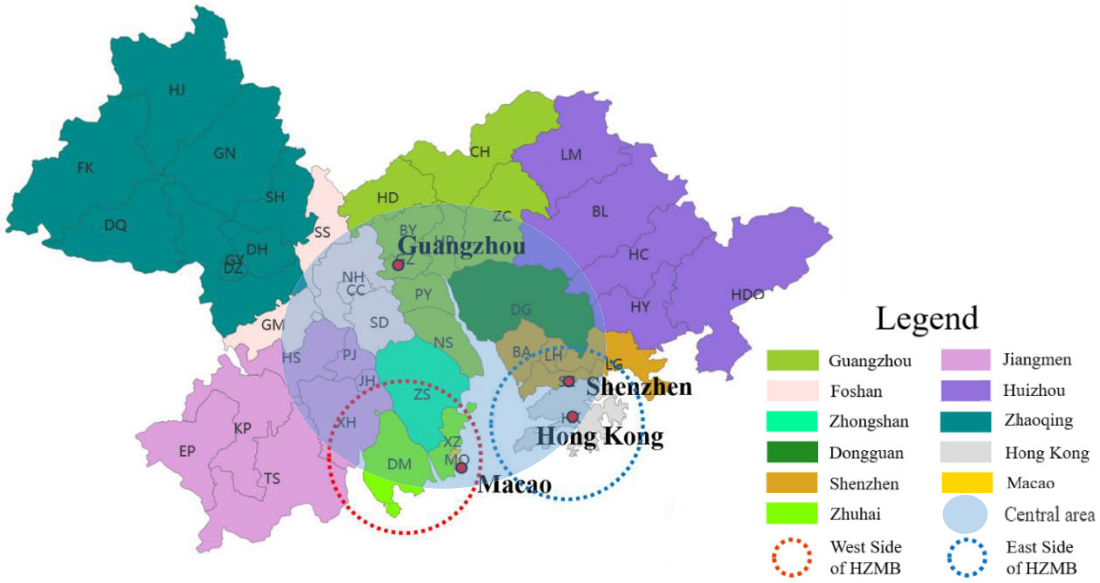

FIGURE 3. Zoning results in the GBA.

TABLE 3. Notation.

Parameter	Interpretation
$\mathcal{I}$	Set of districts, $\mathcal{I} = \{1,2,3,\ldots,I\}$
i,j	Index of district, $i,j \in \mathcal{I}$
α_{ij}	Number of links from district i to district j, $i,j \in \mathcal{I}$
k_i	Node degree of district $i, i \in \mathcal{I}$
$\bar{x}_i$	Average traffic volume starting from district $i,j \in \mathcal{I}$
S_i	Variance of traffic volume starting from district $i, i \in \mathcal{I}$
n	Number of districts in the research area
c_1	Weight of unit area node degree
c_2	Weight of R-mode and Q-mode analysis scores
A_i	Acreage of district $i, i \in \mathcal{I}$
x_{ij}	Traffic flow volume from district i to district $j, i,j \in \mathcal{I}$
x'_{ij}	Revised traffic volume from district i to $j, i,j \in \mathcal{I}$
R_{ij}	Correlation coefficient of traffic volume from district i to district $j, i,j \in \mathcal{I}$
P_k	Percentage of variance quadratic sum for eigenvalue $k \in \mathcal{I}$
P_h	Accumulated percentage of top $p \in \mathcal{I}$ eigenvalues' variance quadratic sum
λ_k	Eigenvalue of each characteristic equation $\lvert \boldsymbol{R} - \lambda_k \boldsymbol{I} \rvert = 0$
$F_{1,i}$	Score of the R-mode analysis of district i
$F_{2,i}$	Score of the Q-mode analysis of district i
M_i	Score of the evaluation in district i

traffic volume from district $i \in \mathcal{J}$ to district $j \in \mathcal{J}$.

$$R_{ij} = \frac{1}{n-1} \sum_{k=1}^{n} x'_{ik} x'_{jk} \quad \forall i, j,\ k \in \mathcal{J} \tag{6}$$

The Jacobi method is used to obtain all eigenvalues and eigenvector matrices. We solve the characteristic equations $|\boldsymbol{R} - \lambda_k \boldsymbol{I}| = 0$, where $\boldsymbol{R}$ denotes the correlation coefficient matrix, and $\boldsymbol{I}$ represents the eigenvector matrices. P_k denotes the percentage of variance quadratic sum of eigenvalue $k \in \mathcal{J}$, and P_h denotes the accumulated percentage of the top $p \in \mathcal{J}$ eigenvalues' variance quadratic sum. Based on the eigenvalues obtained above, each eigenvalue's percentage of the square sum of variance and its accumulated value can be calculated by Equations (7) and (8).

$$P_k = \frac{\lambda_k}{\sum_{k=1}^{n} \lambda_k} \quad k \in \mathcal{J} \tag{7}$$

$$P_h = \frac{\sum_{k=1}^{p} \lambda_k}{\sum_{k=1}^{43} \lambda_k} \quad p \in \mathcal{J} \tag{8}$$

The R-mode analysis and its factors (i.e., P_k, P_h) can reflect traffic agglomeration, while the Q-mode analysis and its extracted factors (i.e., P_k, P_h) can reflect the traffic distribution. The eigenvectors corresponding to the extracted factors are arranged into transformation matrix $\boldsymbol{W}$, and the original matrix $\boldsymbol{A}$ can be calculated by Equation (9), where $\boldsymbol{\Lambda}$ denotes the diagonal matrix composed of eigenvalues.

$$\boldsymbol{A} = \boldsymbol{W}\sqrt{\boldsymbol{\Lambda}} \tag{9}$$

Then, a maximum variance rotation is performed to obtain the factor load matrix after rotation $\boldsymbol{B}$. Based on the matrices obtained above, factor score matrix $\boldsymbol{F}$ can be calculated by Equation (10). Then, the vital R-mode analysis and Q-mode analysis indexes ($F_{1,i}$ and $F_{2,i}$) can be obtained from this matrix.

$$\boldsymbol{F} = \boldsymbol{A}\,(\boldsymbol{\Lambda})^{-2}\boldsymbol{A}'\boldsymbol{X} \tag{10}$$

IV. RESULTS AND DISCUSSION

In this section, we present the results according to the index results from the evaluation model, including the node degree, traffic volume, agglomeration and distribution. We provide some preliminary results of these indices. Then, we discuss the evaluation model and parameter sensitivity analysis.

A. NODE DEGREE

As shown in FIGURE 4, the node degrees of the areas in the GBA dramatically increased from 2018 to 2019 since more new constructed freeways have been introduced for use [1].

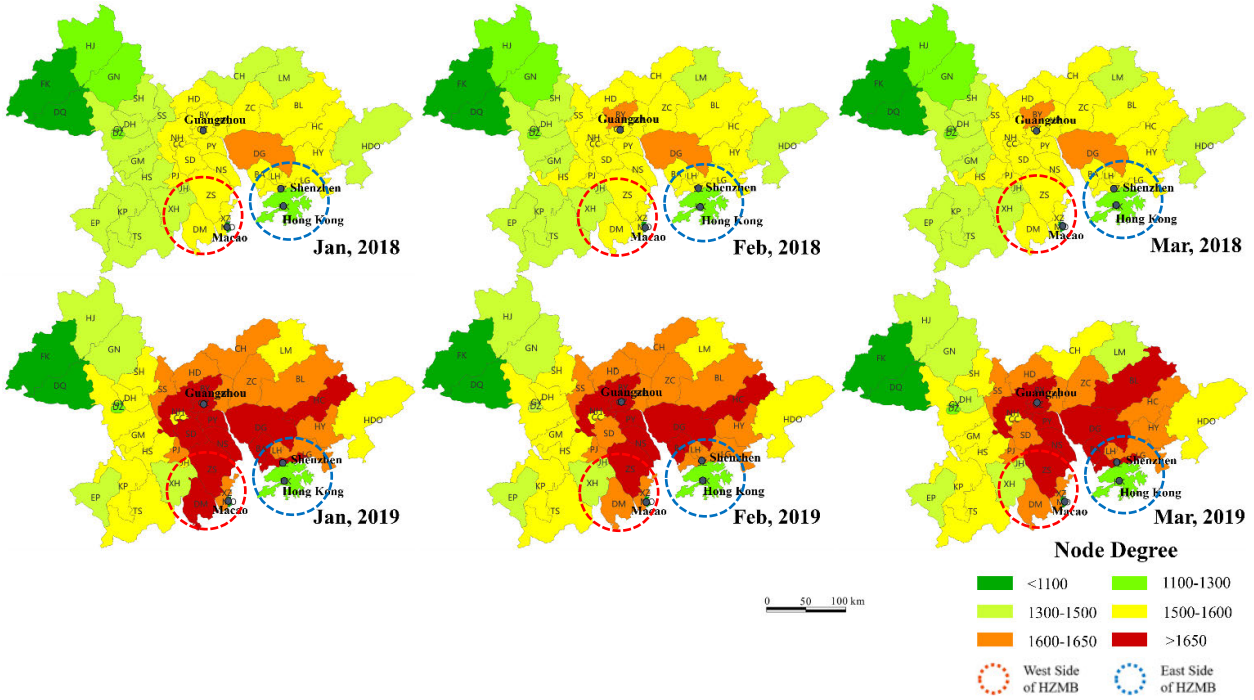

FIGURE 4. Node degree comparison in different areas of the GBA.

TABLE 4. Node degree comparison between the west and east side cities.

HZMB Side	District	Node degree in 2018	Node degree in 2019	Rate Changes	
West	ZS	1578	1666	5.58%	4.95%
	XZ	1528	1614	5.63%	
	DM	1566	1648	5.21%	
	XH	1425	1486	4.26%	
	TS	1447	1519	5.00%	
	MO	826	851	6.15%	
East	SZ	1578	1658	5.10%	4.50%
	BA	1590	1665	4.67%	
	LG	1550	1625	4.82%	
	LH	1534	1625	5.91%	
	HK	1133	1144	0.97%	

In FIGURE 4, the red-colored area has a higher node degree than the green-colored area, and an inverted U-shaped area with a high node degree (in red and dark orange) appeared in 2019. Regarding the degree of all research units, DG ranked in the first position, followed by BY, GZ, BA, PY, ZS, and SZ. Generally, the node degree decreases from the center of the GBA to the edge of the GBA. The node degree of HJ and LM grow the fastest in the GBA with an increased rate of 10.73% and 10.66%, respectively, mainly due to newly built freeways and the HZMB.

As shown in TABLE 4, we compared the node degrees of both sides of the HZMB and their rate changes. On the west side of the HZMB, the average node degree increase rate is 4.95%, which is slightly higher than that in the east side cities.

To better analyze the node degree changes from the time dimension, as shown in FIGURE 5, we compare the node degree of the top three ranked cities (i.e., DG, GZ, and BY) during the period from January to March in

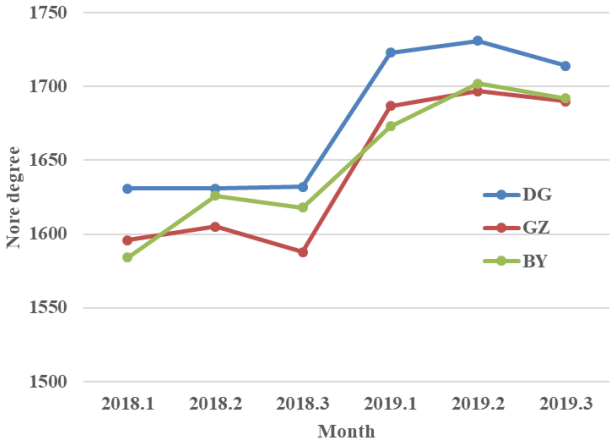

FIGURE 5. Note degree variation over time.

TABLE 5. Node degree in different months.

Area in GBA	District	January	February1*	March
Central area	GZ	1642	1651	1639
	DG	1677	1673	1673
	SZ	1624	1615	1617
Edge area	GN	1326	1415	1304
	HJ	1344	1392	1299
	DQ	977	1066	946

Note: 1*. The Spring Festival occurs in February.
2*. The monthly node degree is the average of the node degree in 2018 and 2019.

2018 and 2019. As shown in TABLE 5, the node degrees of the three top-ranked central areas are over 1600 from

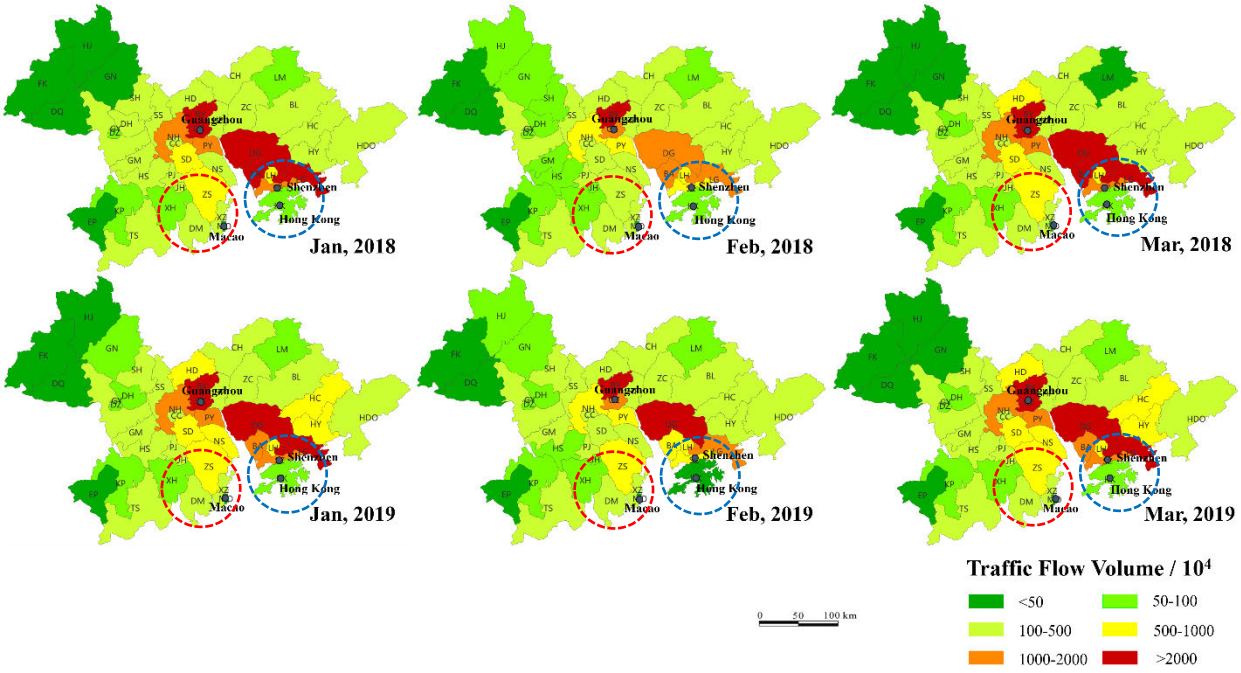

FIGURE 6. Traffic volume in the GBA.

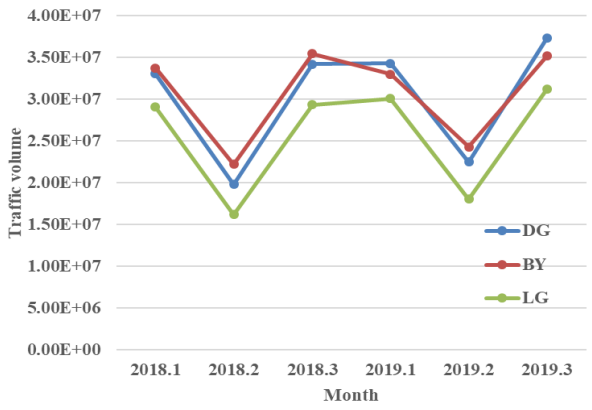

FIGURE 7. Traffic volume/month (top three areas).

TABLE 6. Traffic volume comparison in different months.

Area in GBA	District	January	February1*	March
Central area	GZ	22.21	14.92	23.97
	DG	33.68	21.14	35.76
	SZ	12.16	7.53	12.87
Edge area	GN	0.46	0.59	0.37
	HJ	0.43	0.63	0.34
	DQ	0.24	0.31	0.21

Note: 1*. The Spring Festival is in February

2*. The monthly traffic volume is the average in 2018 and 2019.

TABLE 7. Summary of the traffic volume from the geographical dimension.

HZMB Side	District	Traffic volume in 2018/million	Traffic volume in 2019/million	Rate Changes	
West	ZS	6.20	6.98	12.71%	10.68%
	XZ	2.06	2.46	19.32%	
	DM	3.78	4.11	8.61%	
	XH	0.76	0.76	-0.12%	
	TS	1.45	1.45	0.10%	
	MO	0.07	0.09	20.37%	
East	SZ	10.63	11.07	4.10%	2.02%
	BA	21.47	20.37	-5.15%	
	LG	24.86	26.44	6.37%	
	LH	7.69	8.21	6.72%	
	HK	0.69	0.57	-16.75%	

January to March, and the node degrees in February slightly increase or decrease. The same situation was also observed in the edge GBA areas; the node degrees are approximately 1300, while that in February is slightly higher. February is pretty specially in China since most of the Spring Festival occurs in this month, which could lead to a series of complicated traffic difficulties.

The variation in the note degree occurs for the following two main reasons: civil constructions (e.g., new freeway and bridges that connect more areas) and temporary road closures (e.g., some pavement is under maintenance or reconstruction).

B. TRAFFIC VOLUME

We calculate the traffic volume in the areas of the GBA, and as shown in FIGURE 6, BY, DG, LG, BA and GZ exhibit the highest traffic volume in the GBA. The volume in the different areas significantly varies. In Figure 6, the red-colored area has a higher traffic volume (summation of inflow and outflow volume) than the green-colored area, which formed an inverted U-shaped area in red, orange,

TABLE 8. Results of the R-mode and Q-mode analyses of the GBA.

Number	City	R-mode score		Ranking	Q-mode score		Ranking
		2018	2019	changes	2018	2019	changes
1	GZ	0.806	0.562	-2	0.768	0.689	0
2	BY	0.698	0.7	0	0.739	0.656	0
3	HP	-0.206	-0.215	-1	-0.231	-0.214	1
4	PY	0.204	0.044	-3	0.104	0.114	1
5	NS	-0.102	-0.204	-8	-0.172	-0.173	-1
6	ZC	-0.145	-0.145	-1	-0.141	-0.137	-2
7	HD	-0.173	-0.113	6	-0.177	-0.172	1
8	CH	-0.283	-0.282	-1	-0.283	-0.3	0
9	CC	-0.082	-0.164	-9	-0.116	-0.126	-1
10	NH	0.994	1.111	1	0.982	1.078	0
11	SD	0.249	0.134	-2	0.191	0.148	0
12	GM	-0.201	-0.214	-1	-0.217	-0.196	2
13	SS	0.038	0.089	3	0.021	0.089	2
14	ZS	0.582	0.739	2	0.571	0.61	0
15	DG	1.054	1.105	-1	1.125	1.206	0
16	SZ	-0.029	0.017	1	-0.049	-0.019	1
17	BA	0.353	0.26	0	0.259	0.143	-3
18	LG	0.464	0.489	0	0.338	0.312	0
19	LH	-0.1	-0.066	2	-0.157	-0.127	3
20	XZ	-0.166	-0.113	6	-0.15	-0.118	4
21	DM	-0.145	-0.038	9	0.101	0.096	1
22	PJ	0.141	0.244	2	0.223	0.264	1
23	JH	-0.265	-0.23	3	-0.206	-0.206	-1
24	XH	-0.264	-0.241	-1	-0.206	-0.214	-1
25	TS	-0.315	-0.163	14	-0.156	-0.189	-5
26	KP	-0.099	-0.109	0	-0.129	-0.136	-2
27	EP	-0.237	-0.25	-4	-0.252	-0.25	0
28	HS	-0.223	-0.234	-3	-0.218	-0.223	-1
29	HC	-0.071	-0.143	-7	-0.055	-0.101	-1
30	HY	-0.114	-0.17	-5	-0.109	-0.142	-6
31	HDO	-0.265	-0.314	-6	-0.27	-0.3	-2
32	BL	-0.162	-0.199	-3	-0.165	-0.166	0
33	LM	-0.354	-0.313	1	-0.366	-0.32	0
34	DZ	0.098	0.03	0	0.1	0.06	0
35	DH	0.109	-0.055	-6	0.149	-0.044	-7
36	GN	-0.26	-0.227	1	-0.266	-0.26	0
37	HJ	-0.315	-0.271	3	-0.309	-0.307	-1
38	FK	-0.28	-0.274	-1	-0.31	-0.284	3
39	DQ	-0.179	-0.129	6	-0.195	-0.122	9
40	GY	0.103	0.159	3	0.115	0.207	3
41	SH	-0.083	-0.042	2	-0.075	-0.035	2
42	HK	-0.378	-0.373	0	-0.395	-0.388	0
43	MO	-0.399	-0.393	0	-0.412	-0.404	0

and yellow. Additionally, as shown in this Figure, the traffic volume in February differs from that in January and March. To deeply analyze the differences across these months, FIGURE 7 shows the traffic volume by month.

The traffic volume varies over time, as shown in FIGURE 7, and we calculate the top three traffic volume research areas from January to March in 2018 and 2019. We find that the volumes during the same month steadily increase. Additionally, we find that the traffic volume drastically decreases in February and that the traffic volume in February is only approximately 55% of the traffic volume in January and March. The main reason is the Chinese Spring Festival as many people return to their hometowns and spend more time with their family instead of working. Because of the characteristics of Guangdong province, which has a large number of migrant workers, the traffic volume in February is lower.

To more deeply analyze the top three ranked central areas and edge areas in the GBA (TABLE 6), we find that the traffic volume in the central GBA area (e.g., GZ, DG, and SZ) drastically decreases in February, while the traffic volume in the edge GBA area (e.g., GN, HJ, and DQ) increases in February. This phenomenon may reflect the return home of workers from the central districts of the GBA, and the loss of traffic volume in February suggests that more people in the central GBA gather from other places.

To reflect more geographical characteristics of the GBA area, we also analyze both bridge sides of the HZMB, as shown in TABLE 7. The average increase rate of the west side of the HZMB is 10.68%, which is significantly higher than that of the east side. The reason why the west bank side grows more rapidly than the east bank is complicated. It is believed that the economic downturn in Hong Kong decreased traffic volume.

C. AGGLOMERATION AND DISTRIBUTION RESULTS

Applying the traffic volume data above to Equations (3)-(10), we can finally obtain the R-mode score and Q-mode score of each district, as shown in TABLE 8. TABLE 8 shows the results of the R-mode and Q-mode analyses of the GBA.

TABLE 9. M values of each district in 2018 and 2019 ($c_t = 0.1$, $c_2 = 5$).

City Number	City	2018				2019				Ranking changes
		$\frac{k_i}{A_i}$	$F_{1,i}$	$F_{2,i}$	M_i	$\frac{k_i}{A_i}$	$F_{1,i}$	$F_{2,i}$	M_i	
39	DQ	0.50	-0.18	-0.19	-1.82	0.51	-0.13	-0.12	-1.20	6
25	TS	0.44	-0.31	-0.16	-2.31	0.46	-0.16	-0.19	-1.71	5
20	XZ	2.76	-0.17	-0.15	-1.30	2.91	-0.11	-0.12	-0.86	4
23	JH	12.77	-0.27	-0.21	-1.08	13.15	-0.23	-0.21	-0.86	4
40	GY	0.68	0.10	0.12	1.16	0.72	0.16	0.21	1.91	4
7	HD	1.60	-0.17	-0.18	-1.59	1.69	-0.11	-0.17	-1.26	3
13	SS	1.85	0.04	0.02	0.48	1.96	0.09	0.09	1.09	2
19	LH	8.78	-0.10	-0.16	-0.41	9.27	-0.07	-0.13	-0.04	2
21	DM	1.33	-0.15	0.10	-0.09	1.39	-0.04	0.10	0.43	2
22	PJ	4.79	0.14	0.22	2.30	5.08	0.24	0.26	3.05	2
38	FK	0.35	-0.28	-0.31	-2.92	0.35	-0.27	-0.28	-2.75	2
41	SH	1.18	-0.08	-0.08	-0.67	1.25	-0.04	-0.04	-0.26	2
43	MO	24.36	-0.40	-0.41	-1.62	26.22	-0.39	-0.40	-1.36	2
2	BY	2.04	0.70	0.74	7.39	2.13	0.70	0.66	6.99	1
16	SZ	3.76	-0.03	-0.05	7.53	3.60	0.02	-0.02	7.20	1
36	GN	0.54	-0.26	-0.27	-2.57	0.57	-0.23	-0.26	-2.38	1
37	HJ	0.36	-0.32	-0.31	-3.08	0.40	-0.27	-0.31	-2.85	1
6	ZC	0.96	-0.15	-0.14	-1.34	1.01	-0.14	-0.14	-1.31	0
8	CH	0.77	-0.28	-0.28	-2.75	0.81	-0.28	-0.30	-2.83	0
10	NH	1.47	0.99	0.98	10.03	1.55	1.11	1.08	11.10	0
14	ZS	0.89	0.58	0.57	5.85	0.94	0.74	0.61	6.84	0
15	DG	0.66	1.05	1.12	10.96	0.70	1.11	1.21	11.62	0
18	LG	1.83	0.46	0.34	4.20	1.90	0.49	0.31	4.20	0
33	LM	0.59	-0.35	-0.37	-3.54	0.65	-0.31	-0.32	-3.10	0
42	HK	1.03	-0.38	-0.40	-3.77	1.05	-0.37	-0.39	-3.70	0
3	HP	3.23	-0.21	-0.23	-1.86	3.38	-0.22	-0.21	-1.81	-1
12	GM	1.52	-0.20	-0.22	-1.94	1.63	-0.21	-0.20	-1.89	-1
17	BA	2.89	0.35	0.26	3.35	3.01	0.26	0.14	2.32	-1
24	XH	1.03	-0.26	-0.21	-2.25	1.07	-0.24	-0.21	-2.16	-1
26	KP	0.89	-0.10	-0.13	-1.05	0.93	-0.11	-0.14	-1.13	-1
27	EP	0.81	-0.24	-0.25	-2.36	0.84	-0.25	-0.25	-2.42	-1
28	HS	1.39	-0.22	-0.22	-2.07	1.45	-0.23	-0.22	-2.14	-1
34	DZ	8.01	0.10	0.10	1.79	8.39	0.03	0.06	1.29	-1
1	GZ	5.71	0.81	0.77	8.44	6.06	0.56	0.69	6.86	-3
4	PY	2.02	0.20	0.10	1.74	2.13	0.04	0.11	1.00	-3
11	SD	1.95	0.25	0.19	2.39	2.05	0.13	0.15	1.61	-3
9	CC	9.80	-0.08	-0.12	-0.01	10.22	-0.16	-0.13	-0.43	-3
29	HC	1.04	-0.07	-0.05	-0.52	1.10	-0.14	-0.10	-1.11	-3
31	HDO	0.42	-0.27	-0.27	-2.64	0.45	-0.31	-0.30	-3.03	-3
32	BL	0.54	-0.16	-0.16	-1.58	0.58	-0.20	-0.17	-1.77	-4
35	DH	2.58	0.11	0.15	1.55	2.73	-0.05	-0.04	-0.22	-4
5	NS	2.97	-0.10	-0.17	-1.07	3.14	-0.20	-0.17	-1.57	-5
30	HY	1.68	-0.11	-0.11	-0.95	1.79	-0.17	-0.14	-1.38	-7

DG ranks first in 2018 in the R-mode analysis, followed by NH, GZ, SZ, and BY, while TS, HJ, and LM are low ranking. NH ranks the first in 2019, followed by DG, ZS, BY and SZ. In the Q-mode analysis, DG ranked the first in both 2018 and 2019, while NH, GZ, SZ, and BY are also high ranking.

After the opening of the HZMB, the agglomeration function of the west side of the HZMB improved as follows: ZS, XZ, and DM climbed 3, 6, and 9 ranks, respectively, and TS even climbed 14 ranks, but the results of the Q-mode analysis changed to a lesser degree, indicating that the agglomeration function of the HZMB is much stronger than the distribution function and that the west side of the HZMB benefits more from the bridge than the east side. However, the agglomeration and distribution functions of the bridge will gradually balance according to FIGURE 2 since the vehicle quota policy is generally liberalized.

Notably, the fastest-growing district is DQ likely due to the newly built freeway. The new freeway not only results in a better distribution function in DQ, FK, and other districts in Zhaoqing but also provides a more convenient choice for the districts above to travel to the central GBA.

D. MODEL RESULTS

By applying the results of the node degree analysis and agglomeration and distribution analysis to Equation (1), we can obtain the model results, as shown in TABLE 9.

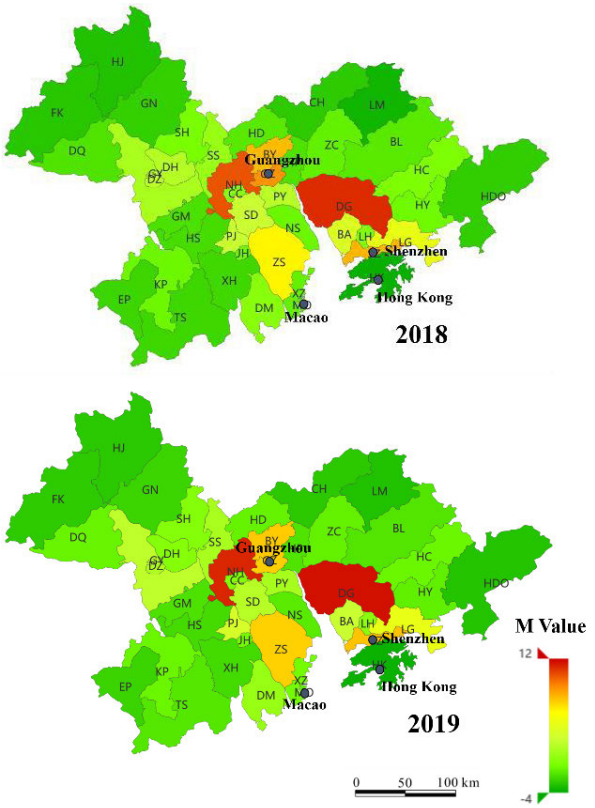

FIGURE 8. M values of each district in 2018 and 2019.

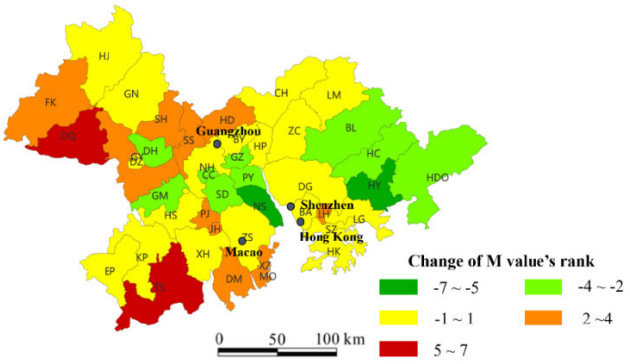

FIGURE 9. Changes in the *M* value rankings from 2018 to 2019.

TABLE 10. Urban hierarchical results.

Traffic hub city level	Average Score	Included	Characteristics
Level-1	⩾5	DG, NH, GZ, SZ, BY, ZS	1. Dense freeway network and active traffic 2. Influencing areas cover the entire GBA
Level-2	0-5	PY, SD, BA, LG, PJ, DZ, DH, GY	1. Good traffic infrastructure 2. Influencing areas are smaller than the GBA traffic hub cities
Level-3	<0	Remaining cities	1. Weak traffic agglomeration and distribution function 2. Use the hub cities' infrastructure to agglomerate and distribute

TABLE 9 presents the M value of each district in 2018 and 2019 in the hub city evaluation model. Considering the difference in magnitude between the unit area node degree and the score of the R-mode and Q-mode analyses, we choose 0.1 and 5 as the values of parameters c_1 and c_2, respectively.

FIGURE 8 shows the M values of all research units in 2018 and 2019. The values of DG, NH, SZ, GZ, BY, and ZS are relatively high within the GBA in 2018 and 2019, suggesting that these districts are traffic hub cities in the GBA. DG, which is located between GZ and SZ, exhibits the highest centrality and has a vital traffic effect in the GBA. Additionally, NH, GZ, and BY can be hub cities in the Guangzhou-Foshan-Zhaoqing urban agglomeration, DG and SZ can be hub cities in the Shenzhen-Dongguan-Huizhou urban agglomeration, and ZS can be a hub city in the Zhuhai-Zhongshan-Jiangmen urban agglomeration. FIGURE 9 shows the ranking changes in these areas. As shown in the figure, the M value rank drastically increases in the west side areas of the HZMB and the districts in Zhaoqing. In the former area, the TS, XZ, DM, and MO rankings rise mainly due to the HZMB. In the latter area, the DQ, GY, SH, and FK rankings increase due to the newly built Guangzhou-Foshan-Zhaoqing Freeway. We can obtain further information from FIGURE 6, which shows that the western GBA's M values change more rapidly, indicating that the government invests more in the infrastructure of the western GBA. However, there is not much improvement in the transportation infrastructure in the districts in HZ and GZ, leading to a decline in their rankings.

E. SENSITIVITY ANALYSIS

Based on the model results, we change parameters c_1 and c_2 to carry out a sensitivity analysis, and the detailed results are shown in FIGURE 10. With the growing ratio of c_2 to c_1 (i.e., c_2/c_1), the differences between the M values of different districts become increasingly apparent.

When the ratio is 1, suggesting that the unit area node degree is as significant as the score of the agglomeration and distribution analysis, the M value of most districts is approximately 0, and the differences are small. It is inconvenient to carry out a hub city analysis and classification based on these data. When the ratio reaches 100, suggesting that the score of the agglomeration and distribution analysis is the main influencing factor, the differences among the districts become very significant. However, in this ratio, districts with small acreages, such as CC, JH, and MO, have low M values, while the M values of districts with large acreages are relatively high. In this ratio, the function of the unit area node degree is ignored, but the function of the agglomeration and distribution analysis is enlarged. When the ratio is 50, which is the medium between 1 and 100, the results are not only definite but also consider both the node degree results and agglomeration and distribution results. In addition, when c_2/c_1 is 50, the M values are the closest to the average M values when c_2/c_1 ranges from 1 to 100.

As shown in TABLE 11, GBA traffic hub cities have a dense freeway network and active traffic agglomeration and distribution; the regional traffic hub cities' influencing areas

	$\frac{C_2}{C_1}$	1	5	10	15	20	25	30	35	40	45	50	55	60	65	70	75	80	85	90	95	100	Average
Level-1	DG	0.28	1.16	2.24	3.33	4.42	5.51	6.60	7.69	8.78	9.87	10.96	12.05	13.14	14.23	15.32	16.40	17.49	18.58	19.67	20.76	21.85	10.97
	NH	0.34	1.14	2.12	3.11	4.10	5.09	6.08	7.07	8.05	9.04	10.03	11.02	12.01	12.99	13.98	14.97	15.96	16.95	17.94	18.92	19.91	10.04
	GZ	0.73	1.36	2.14	2.93	3.72	4.51	5.29	6.08	6.87	7.65	8.44	9.23	10.01	10.80	11.59	12.37	13.16	13.95	14.74	15.52	16.31	8.45
	SZ	0.52	1.09	1.81	2.52	3.24	3.95	4.67	5.38	6.10	6.81	7.53	8.24	8.96	9.67	10.39	11.10	11.82	12.53	13.25	13.96	14.68	7.53
	BY	0.35	0.92	1.64	2.36	3.08	3.80	4.52	5.23	5.95	6.67	7.39	8.11	8.83	9.55	10.27	10.98	11.70	12.42	13.14	13.86	14.58	7.40
	ZS	0.20	0.67	1.24	1.82	2.40	2.97	3.55	4.12	4.70	5.28	5.85	6.43	7.01	7.58	8.16	8.74	9.31	9.89	10.47	11.04	11.62	5.86
Level-2	LG	0.26	0.58	0.99	1.39	1.79	2.19	2.59	2.99	3.39	3.79	4.20	4.60	5.00	5.40	5.80	6.20	6.60	7.00	7.40	7.81	8.21	4.20
	BA	0.35	0.59	0.90	1.21	1.51	1.82	2.12	2.43	2.74	3.04	3.35	3.65	3.96	4.27	4.57	4.88	5.18	5.49	5.79	6.10	6.41	3.35
	SD	0.24	0.41	0.63	0.85	1.07	1.29	1.51	1.73	1.95	2.17	2.39	2.61	2.83	3.05	3.27	3.49	3.71	3.93	4.15	4.37	4.59	2.39
	PJ	0.52	0.66	0.84	1.03	1.21	1.39	1.57	1.76	1.94	2.12	2.30	2.49	2.67	2.85	3.03	3.21	3.40	3.58	3.76	3.94	4.13	2.30
	DZ	0.82	0.90	1.00	1.10	1.20	1.29	1.39	1.49	1.59	1.69	1.79	1.89	1.99	2.08	2.18	2.28	2.38	2.48	2.58	2.68	2.78	1.79
	PY	0.23	0.36	0.51	0.66	0.82	0.97	1.13	1.28	1.43	1.59	1.74	1.90	2.05	2.21	2.36	2.51	2.67	2.82	2.98	3.13	3.28	1.74
	DH	0.28	0.39	0.52	0.65	0.77	0.90	1.03	1.16	1.29	1.42	1.55	1.68	1.81	1.93	2.06	2.19	2.32	2.45	2.58	2.71	2.84	1.55
	GY	0.09	0.18	0.29	0.40	0.51	0.62	0.72	0.83	0.94	1.05	1.16	1.27	1.38	1.49	1.60	1.71	1.82	1.93	2.04	2.15	2.26	1.16
	SS	0.19	0.21	0.24	0.27	0.30	0.33	0.36	0.39	0.42	0.45	0.48	0.51	0.53	0.56	0.59	0.62	0.65	0.68	0.71	0.74	0.77	0.48
Level-3	CC	0.96	0.88	0.78	0.68	0.58	0.49	0.39	0.29	0.19	0.09	-0.01	-0.11	-0.21	-0.30	-0.40	-0.50	-0.60	-0.70	-0.80	-0.90	-1.00	-0.01
	DM	0.13	0.11	0.09	0.07	0.04	0.02	0.00	-0.02	-0.04	-0.07	-0.09	-0.11	-0.13	-0.15	-0.18	-0.20	-0.22	-0.24	-0.27	-0.29	-0.31	-0.09
	LH	0.85	0.75	0.62	0.49	0.36	0.24	0.11	-0.02	-0.15	-0.28	-0.41	-0.54	-0.66	-0.79	-0.92	-1.05	-1.18	-1.31	-1.44	-1.56	-1.69	-0.41
	HC	0.09	0.04	-0.02	-0.08	-0.15	-0.21	-0.27	-0.33	-0.40	-0.46	-0.52	-0.59	-0.65	-0.71	-0.77	-0.84	-0.90	-0.96	-1.02	-1.09	-1.15	-0.52
	SH	0.10	0.04	-0.04	-0.12	-0.20	-0.28	-0.35	-0.43	-0.51	-0.59	-0.67	-0.75	-0.83	-0.91	-0.99	-1.06	-1.14	-1.22	-1.30	-1.38	-1.46	-0.67
	HY	0.15	0.06	-0.05	-0.17	-0.28	-0.39	-0.50	-0.61	-0.72	-0.83	-0.95	-1.06	-1.17	-1.28	-1.39	-1.50	-1.61	-1.73	-1.84	-1.95	-2.06	-0.95
	KP	0.07	-0.03	-0.14	-0.25	-0.37	-0.48	-0.60	-0.71	-0.82	-0.94	-1.05	-1.16	-1.28	-1.39	-1.51	-1.62	-1.73	-1.85	-1.96	-2.08	-2.19	-1.05
	NS	0.27	0.16	0.02	-0.11	-0.25	-0.39	-0.52	-0.66	-0.80	-0.94	-1.07	-1.21	-1.35	-1.48	-1.62	-1.76	-1.89	-2.03	-2.17	-2.31	-2.44	-1.07
	JH	1.23	1.04	0.81	0.57	0.33	0.10	-0.14	-0.37	-0.61	-0.84	-1.08	-1.31	-1.55	-1.79	-2.02	-2.26	-2.49	-2.73	-2.96	-3.20	-3.43	-1.08
	XZ	0.24	0.12	-0.04	-0.20	-0.36	-0.51	-0.67	-0.83	-0.99	-1.15	-1.30	-1.46	-1.62	-1.78	-1.94	-2.09	-2.25	-2.41	-2.57	-2.73	-2.89	-1.31
	ZC	0.07	-0.05	-0.19	-0.33	-0.48	-0.62	-0.76	-0.91	-1.05	-1.19	-1.34	-1.48	-1.62	-1.76	-1.91	-2.05	-2.19	-2.34	-2.48	-2.62	-2.77	-1.34
	BL	0.02	-0.11	-0.27	-0.44	-0.60	-0.76	-0.93	-1.09	-1.25	-1.42	-1.58	-1.74	-1.91	-2.07	-2.23	-2.40	-2.56	-2.72	-2.89	-3.05	-3.21	-1.58
	HD	0.12	-0.01	-0.19	-0.36	-0.54	-0.71	-0.89	-1.06	-1.24	-1.41	-1.59	-1.76	-1.94	-2.11	-2.29	-2.46	-2.64	-2.81	-2.99	-3.16	-3.33	-1.59
	MO	2.35	2.03	1.63	1.22	0.82	0.41	0.01	-0.40	-0.81	-1.21	-1.62	-2.02	-2.43	-2.83	-3.24	-3.64	-4.05	-4.45	-4.86	-5.26	-5.67	-1.62
	DQ	0.01	-0.14	-0.32	-0.51	-0.70	-0.88	-1.07	-1.26	-1.44	-1.63	-1.82	-2.00	-2.19	-2.38	-2.56	-2.75	-2.94	-3.12	-3.31	-3.50	-3.69	-1.82
	HP	0.28	0.10	-0.11	-0.33	-0.55	-0.77	-0.99	-1.20	-1.42	-1.64	-1.86	-2.08	-2.29	-2.51	-2.73	-2.95	-3.17	-3.38	-3.60	-3.82	-4.04	-1.86
	GM	0.11	-0.06	-0.27	-0.47	-0.68	-0.89	-1.10	-1.31	-1.52	-1.73	-1.94	-2.15	-2.36	-2.57	-2.78	-2.98	-3.19	-3.40	-3.61	-3.82	-4.03	-1.94
	HS	0.09	-0.08	-0.30	-0.52	-0.74	-0.96	-1.19	-1.41	-1.63	-1.85	-2.07	-2.29	-2.51	-2.73	-2.95	-3.17	-3.39	-3.61	-3.83	-4.06	-4.28	-2.07
	XH	0.06	-0.13	-0.37	-0.60	-0.84	-1.07	-1.31	-1.54	-1.78	-2.01	-2.25	-2.49	-2.72	-2.96	-3.19	-3.43	-3.66	-3.90	-4.13	-4.37	-4.60	-2.25
	TS	0.00	-0.19	-0.43	-0.66	-0.90	-1.13	-1.37	-1.60	-1.84	-2.07	-2.31	-2.55	-2.78	-3.02	-3.25	-3.49	-3.72	-3.96	-4.19	-4.43	-4.66	-2.31
	BP	0.03	-0.16	-0.41	-0.65	-0.90	-1.14	-1.39	-1.63	-1.87	-2.12	-2.36	-2.61	-2.85	-3.10	-3.34	-3.59	-3.83	-4.08	-4.32	-4.56	-4.81	-2.37
	GN	0.00	-0.21	-0.47	-0.73	-1.00	-1.26	-1.52	-1.79	-2.05	-2.31	-2.57	-2.84	-3.10	-3.36	-3.63	-3.89	-4.15	-4.41	-4.68	-4.94	-5.20	-2.58
	HDO	-0.01	-0.23	-0.49	-0.76	-1.03	-1.30	-1.56	-1.83	-2.10	-2.37	-2.64	-2.90	-3.17	-3.44	-3.71	-3.97	-4.24	-4.51	-4.78	-5.05	-5.31	-2.64
	CH	0.02	-0.21	-0.49	-0.77	-1.05	-1.34	-1.62	-1.90	-2.18	-2.47	-2.75	-3.03	-3.32	-3.60	-3.88	-4.16	-4.45	-4.73	-5.01	-5.29	-5.58	-2.75
	FK	-0.02	-0.26	-0.55	-0.85	-1.14	-1.44	-1.73	-2.03	-2.33	-2.62	-2.92	-3.21	-3.51	-3.80	-4.10	-4.39	-4.69	-4.98	-5.28	-5.57	-5.87	-2.92
	HJ	-0.03	-0.28	-0.59	-0.90	-1.21	-1.52	-1.84	-2.15	-2.46	-2.77	-3.08	-3.40	-3.71	-4.02	-4.33	-4.64	-4.96	-5.27	-5.58	-5.89	-6.21	-3.09
	LM	-0.01	-0.30	-0.66	-1.02	-1.38	-1.74	-2.10	-2.46	-2.82	-3.18	-3.54	-3.90	-4.26	-4.62	-4.98	-5.34	-5.70	-6.06	-6.42	-6.78	-7.14	-3.54
	HK	0.03	-0.28	-0.67	-1.06	-1.44	-1.83	-2.22	-2.60	-2.99	-3.38	-3.77	-4.15	-4.54	-4.93	-5.31	-5.70	-6.09	-6.47	-6.86	-7.25	-7.63	-3.77

FIGURE 10. Results of the sensitivity analysis.

are mainly the adjacent districts, and the influence of the first type of cities is smaller, while normal cities have the weakest traffic agglomeration and distribution function and usually agglomerate and distribute traffic through the infrastructure of hub cities. According to the average score of the sensitivity analysis, we can divide the 43 districts into three types according to the central place theory and urban hierarchical theory proposed by Christaller [63]. As shown in TABLE 11, the proportions of the three types of districts, which are called Level-1 to Level 3 traffic hub cities, are 15%, 20%, and 65%.

We also find that the hub cities are mainly located at the center of the GBA and perform better economically than other districts. Thus, the geographical location, traffic centrality, and economic performance of a city are interrelated, and an advantageous geographical location creates superior traffic centrality, thus leading to high economic performance.

V. CONCLUSION

Using a full sample of freeway toll data, this paper proposes an evaluation model to explore the traffic operation and determine the hub traffic cities in the GBA before and after the HZMB opened to traffic. By using the methodology of the node degree, traffic volume, and agglomeration and distribution theory, we reach some conclusions.

First, the west side of the HZMB benefits more from the bridge than the east side, and the agglomeration function of the HZMB is much stronger than the distribution function. The analysis of the node degree and traffic volume shows that the west side (ZS, XZ, DM, XH, TS, and MO) is rapidly rising. Based on the results of the agglomeration and distribution analysis, we discover that the ranking changes more drastically in terms of agglomeration than in terms of distribution after the opening of the HZMB. This situation occurs because the HZMB is mainly used for leisure and sightseeing rather than for transportation and commuting.

Second, the urban hierarchical pattern and hub cities in the GBA are clear. Six districts (i.e., DG, NH, GZ, SZ, BY, and ZS) are Level-1 traffic hub cities, and nine districts (i.e., PY, SD, BA, LG, PJ, DZ, DH, and GY) include Level-2 traffic hub cities. These hub cities exhibit sound traffic infrastructure and play an essential role in agglomerating and distributing the traffic in the GBA. Integrating resources in the GBA and accelerating the transfer of logistics, business, and information flow with the help of the convenient transportation infrastructure of the hub cities is vital for group development.

The model proposed in this paper has great application value and can help reflect the communication among districts through traffic data, predict the development trend of the social economy, and guide urban agglomeration planning. However, the use of freeway data alone cannot provide a complete assessment of the regional development level and the economic benefits of the HZMB. In the future, multisource and long-term data will be considered, and data offered by the HZMB Authority will also be emphasized in analyses. Moreover, we will apply more sophisticated models to reflect the economic and traffic development of the GBA.

REFERENCES

[1] *Guangdong Statistical Yearbook*, Statist. Bureau Guangdong Province, Guangzhou, China, 2018.

[2] C. Yang, Q. Li, Z. Hu, J. Chen, T. Shi, K. Ding, and G. Wu, "Spatiotemporal evolution of urban agglomerations in four major bay areas of US, China and Japan from 1987 to 2017: Evidence from remote sensing images," *Sci. Total Environ.*, vol. 671, pp. 232–247, Jun. 2019.

[3] F. Peng, "Economic spatial connection and spatial structure of Guangdong-Hong Kong-Macao Greater Bay and the surrounding area cities—An empirical analysis based on improved gravity model and social network analysis," *Econ. Geography.*, vol. 37, no. 12, pp. 57–64, 2017.

[4] X. Cao, S. Ouyang, W. Yang, Y. Luo, B. Li, and D. Liu, "Transport accessibility and spatial connections of cities in the Guangdong-Hong Kong-Macao greater bay area," *Chin. Geogrph. Sci.*, vol. 29, no. 5, pp. 820–833, Oct. 2019.

[5] S. M. Kowleski, "Golden gate coordinated system-commuting by land and by sea," SAE Tech. Papers 760625, 1976.

[6] M. Du, D. Zellers, J. Wang, F. Pepe, and C. Saladino, "New bronx-whitestone Bridge approach foundations design and construction," in *Proc. IFCEE*, Jun. 2018, pp. 196–211.

[7] N. M. Macek, A. J. Khattak, and R. G. Quercia, "What is the effect of commute time on employment?: Analysis of spatial patterns in New York metropolitan area," *Transp. Res. Rec.*, vol. 1780, no. 1, pp. 43–52, Jan. 2001.

[8] L. Montemayor and E. Calvin, "Identification and classification of urban development place types for the New York metropolitan region," in *Proc. 1st Int. ACM SIGSPATIAL Workshop Smart Cities Urban Analytics (UrbanGIS)*, 2015, pp. 101–106.

[9] P. A. Viton, "On competition and product differentiation in urban transportation: The San Francisco Bay Area," *Bell J. Econ.*, vol. 12, no. 2, p. 362, 1981.

[10] M. J. Santos, J. H. Thorne, J. Christensen, and Z. Frank, "An historical land conservation analysis in the San Francisco Bay Area, USA: 1850–2010," *Landscape Urban Planning*, vol. 127, pp. 114–123, Jul. 2014.

[11] A. J. Khattak and Y. Yim, "Traveler response to innovative personalized demand-responsive transit in the San Francisco Bay Area," *J. Urban Plann. Dev.*, vol. 130, no. 1, pp. 42–55, Mar. 2004.

[12] H. Kato, D. Fukuda, Y. Yamashita, S. Iwakura, and T. Yai, "Latest urban rail demand forecast model system in the Tokyo Metropolitan Area," *Transp. Res. Rec.*, vol. 2668, no. 1, pp. 60–77, Jan. 2017.

[13] R. Abe, "Introducing autonomous buses and taxis: Quantifying the potential benefits in Japanese transportation systems," *Transp. Res. A, Policy Pract.*, vol. 126, pp. 94–113, Aug. 2019.

[14] W. Liu, J. Zhan, F. Zhao, H. Yan, F. Zhang, and X. Wei, "Impacts of urbanization-induced land-use changes on ecosystem services: A case study of the Pearl River Delta Metropolitan Region, China," *Ecological Indicators*, vol. 98, pp. 228–238, Mar. 2019.

[15] X. Lu and Q. Liu, "Study on optimization of regional spatial structure based on land use and transport accessibility: A case study of Pearl River Delta region," *Appl. Mech. Mater.*, vol. 137, pp. 435–439, Oct. 2011.

[16] Z. Wu, J. D. Milliman, D. Zhao, Z. Cao, J. Zhou, and C. Zhou, "Geomorphologic changes in the lower Pearl River Delta, 1850–2015, largely due to human activity," *Geomorphology*, vol. 314, pp. 42–54, Aug. 2018.

[17] Z. Wu, J. D. Milliman, D. Zhao, J. Zhou, and C. Yao, "Recent geomorphic change in LingDing Bay, China, in response to economic and urban growth on the Pearl River Delta, Southern China," *Global Planet. Change*, vol. 123, pp. 1–12, Dec. 2014.

[18] J. Dai, Z.-D. Xu, X.-J. Yin, P.-P. Gai, and Y. Luo, "Parameters design of TMD mitigating vortex-induced vibration of the Hong Kong–Zhuhai–Macao Bridge deep-water nonnavigable Bridge," *J. Bridge Eng.*, vol. 24, no. 8, Aug. 2019, Art. no. 06019005.

[19] W. Duan, G. Cai, S. Liu, Y. Du, L. Zhu, and A. J. Puppala, "SPT–CPTU correlations and liquefaction evaluation for the island and tunnel project of the Hong Kong–Zhuhai–Macao Bridge," *Int. J. Civil Eng.*, vol. 16, no. 10, pp. 1423–1434, Oct. 2018, doi: 10.1007/s40999-017-0281-9.

[20] Q. Hou and S.-M. Li, "Transport infrastructure development and changing spatial accessibility in the Greater Pearl River Delta, China, 1990–2020," *J. Transport Geography*, vol. 19, no. 6, pp. 1350–1360, Nov. 2011.

[21] Y. Song, "The strategy of Hong Kong-Zhuhai-Macao economic integration development under the background of Hong Kong-Zhuhai-Macao Bridge," in *Proc. 3rd Int. Conf. Contemp. Edu., Social Sci. Humanities (ICCESSH)*, 2018, pp. 955–958.

[22] H. Liu, *Analysis of the Influence of Hong Kong Zhuhai Macao Bridge on Regional Development and Transportation*. Guangdong Province, China: South China Univ. of Technology, 2010.

[23] M. E. J. Newman, "Scientific collaboration networks. II. Shortest paths, weighted networks, and centrality," *Phys. Rev. E, Stat. Phys. Plasmas Fluids Relat. Interdiscip. Top.*, vol. 73, no. 3, 2006, Art. no. 039906.

[24] D. Gomez, E. González-Arangüena, C. Manuel, G. Owen, M. del Pozo, and J. Tejada, "Centrality and power in social networks: A game theoretic approach," *Math. Social Sci.*, vol. 46, no. 1, pp. 39–40, 2003.

[25] A. P. Masucci, K. Stanilov, and M. Batty, "Exploring the evolution of London's street network in the information space: A dual approach," *Phys. Rev. E, Stat. Phys. Plasmas Fluids Relat. Interdiscip. Top.*, vol. 89, no. 1, 2014, Art. no. 012805.

[26] M. Sánchez-Silva, M. Daniels, G. Lleras, and D. Patiño, "A transport network reliability model for the efficient assignment of resources," *Transp. Res. B, Methodol.*, vol. 39, no. 1, pp. 47–63, Jan. 2005.

[27] M. Li, H. Wang, and H. Wang, "Resilience assessment and optimization for urban rail transit networks: A case study of beijing subway network," *IEEE Access*, vol. 7, pp. 71221–71234, 2019.

[28] X. Ai, "New metrics for node importance evaluation in occupational injury network," *IEEE Access*, vol. 7, pp. 61874–61882, 2019.

[29] L. Wang, L. Wei, Y. Z. Zhang, and Z. X. Li, "Node importance assessment of traffic complex network based on C-means clustering," *Adv. Mater. Res.*, vols. 211–212, pp. 963–967, Feb. 2011.

[30] H. Tamura, M. Koppen, M. Uchida, M. Tsuru, and Y. Oie, "Node degree-aware link cost for traffic load-distribution in large-scale networks," in *Proc. 3rd Int. Conf. Intell. Netw. Collaborative Syst.*, Nov. 2011, pp. 299–304.

[31] J. Shimada, H. Tamura, M. Uchida, and Y. Oie, "Node degree based routing metric for traffic load distribution in the Internet," *IEICE Trans. Inf. Syst.*, vol. E96.D, no. 2, pp. 202–212, 2013.

[32] H. Tamura, M. Uchida, M. Tsuru, J. Shimada, T. Ikenaga, and Y. Oie, "Routing metric based on node degree for load-balancing in large-scale networks," in *Proc. IEEE/IPSJ Int. Symp. Appl. Internet*, Jul. 2011, pp. 519–523.

[33] Z. Liu, X. Zhang, Y. Zhao, and H. Guan, "An asymptotically minimal node-degree topology for load-balanced architectures," in *Proc. IEEE Global Telecommun. Conf. (IEEE GLOBECOM)*, Nov./Dec. 2008, pp. 1–6.

[34] Z. Kong and E. Yeh, "Wireless network resilience to degree-dependent and cascading node failures," in *Proc. 7th Int. Symp. Modeling Optim. Mobile, Ad Hoc, Wireless Netw.*, Jun. 2009.

[35] S. Meloni, J. Gómez-Gardeñes, V. Latora, and Y. Moreno, "Effects of traffic properties and degree heterogeneity in flow fluctuations on complex networks," *Int. J. Bifurcation Chaos*, vol. 22, no. 07, Jul. 2012, Art. no. 1250170.

[36] L. Lin, K. Yuan, and S. Ren, "Analysis of urban freeway traffic flow characteristics based on frequent pattern tree," in *Proc. 17th Int. IEEE Conf. Intell. Transp. Syst. (ITSC)*, Oct. 2014, pp. 1719–1725.

[37] Z. Khan, S. M. Khan, K. Dey, and M. Chowdhury, "Development and evaluation of recurrent neural network-based models for hourly traffic volume and annual average daily traffic prediction," *Transp. Res. Rec.*, vol. 2673, no. 7, pp. 489–503, Jul. 2019.

[38] T. Wang, B. Hu, K. Xie, J. Li, G. Song, and L. Chu, "Relationship on traffic volume of urban, suburban and outside city of Beijing expressway," in *Proc. Int. Conf. Mechanic Autom. Control Eng.*, Jun. 2010, pp. 4963–4966.

[39] K. Lewin, *Field Theory in Social Science*. New York, NY, USA: Harper and Brother Publisher, 1951.

[40] B. J. L. Berry, "Interdependency of spatial structure and spatial behavior: A general field theory formulation," *Papers Regional Sci.*, vol. 21, no. 1, pp. 205–227, Jul. 2010.
[41] A. W. Veenstra, H. M. Mulder, and R. A. Sels, "Analysing container flows in the Caribbean," *J. Transp. Geography*, vol. 13, no. 4, pp. 295–305, Dec. 2005.
[42] M. Jansen-Verbeke and R. Spee, "A regional analysis of tourist flows within Europe," *Tourism Manage.*, vol. 16, no. 1, pp. 73–80, Feb. 1995.
[43] T. Hong, T. Ma, and T.-C. Huan, "Network behavior as driving forces for tourism flows," *J. Bus. Res.*, vol. 68, no. 1, pp. 146–156, Jan. 2015, doi: 10.1016/j.jbusres.2014.04.006.
[44] S. Baoyan and W. Li'e, "The functional structure evolution of Shandong Peninsula Urban Agglomeration," in *Proc. IEEE Int. Conf. Cloud Comput. Big Data Anal. (ICCCBDA)*, Jul. 2016, pp. 97–101.
[45] R. Han, H. Cao, and Z. Liu, "Studying the urban hierarchical pattern and spatial structure of China using a synthesized gravity model," *Sci. China Earth Sci.*, vol. 61, no. 12, pp. 1818–1831, Dec. 2018.
[46] M. Jain and A. Korzhenevych, "Detection of urban system in India: Urban hierarchy revisited," *Landscape Urban Planning*, vol. 190, Oct. 2019, Art. no. 103588, doi: 10.1016/j.landurbplan.2019.103588.
[47] W. Yue, S. Qiu, H. Xu, L. Xu, and L. Zhang, "Polycentric urban development and urban thermal environment: A case of Hangzhou, China," *Landscape Urban Planning*, vol. 189, pp. 58–70, Sep. 2019, doi: 10.1016/j.landurbplan.2019.04.008.
[48] B. Wu, B. Yu, S. Yao, Q. Wu, Z. Chen, and J. Wu, "A surface network based method for studying urban hierarchies by night time light remote sensing data," *Int. J. Geograph. Inf. Sci.*, vol. 33, no. 7, pp. 1377–1398, Jul. 2019, doi: 10.1080/13658816.2019.1585540.
[49] A. De Montis, M. Barthélemy, A. Chessa, and A. Vespignani, "The structure of interurban traffic: A weighted network analysis," *Environ. Planning B, Urban Anal. City Sci.*, vol. 34, no. 5, pp. 905–924, Oct. 2007.
[50] M. Knudsen and J. Rich, "Ex post socio-economic assessment of the Oresund Bridge," *Transp. Policy*, vol. 27, pp. 53–65, May 2013.
[51] Q. Wu, Y. Li, and H. Zhang, "Spatial accessibility effect of the Shenzhen-Zhongshan Bridge in Pearl River Delta, China," in *Proc. Asia–Pacific Conf. Intell. Med. Int. Conf. Transp. Traffic Eng. (APCIM & ICTTE)*, 2018, pp. 268–272.
[52] S. Xiao, X. C. Liu, and Y. Wang, "Data-driven geospatial-enabled transportation platform for freeway performance analysis," *IEEE Intell. Transp. Syst. Mag.*, vol. 7, no. 2, pp. 10–21, Apr. 2015.
[53] X. Ma and Y. Wang, "Development of a data-driven platform for transit performance measures using smart card and GPS data," *J. Transp. Eng.*, vol. 140, no. 12, Dec. 2014, Art. no. 04014063.
[54] S. Sharma, Y. Cui, Q. He, R. Mohammadi, and Z. Li, "Data-driven optimization of railway maintenance for track geometry," *Transp. Res. C, Emerg. Technol.*, vol. 90, pp. 34–58, May 2018.
[55] F. Ghofrani, Q. He, R. M. Goverde, and X. Liu, "Recent applications of big data analytics in railway transportation systems: A survey," *Transp. Res. C, Emerg. Technol.*, vol. 90, pp. 226–246, May 2018.
[56] T. S. J. Darwish and K. Abu Bakar, "Fog based intelligent transportation big data analytics in the Internet of vehicles environment: Motivations, architecture, challenges, and critical issues," *IEEE Access*, vol. 6, pp. 15679–15701, 2018.
[57] C. Badii, P. Nesi, and I. Paoli, "Predicting available parking slots on critical and regular services by exploiting a range of open data," *IEEE Access*, vol. 6, pp. 44059–44071, 2018.
[58] L. Guo, H. Xu, and K. Harfoush, "The node degree for wireless ad hoc networks in shadow fading environments," in *Proc. 6th IEEE Conf. Ind. Electron. Appl.*, Jun. 2011, pp. 815–820.
[59] H. Li, Y. Zhao, J. Bai, J. Zhang, and J. Yang, "Comparative study in complex network: Node degree and topological potential," in *Proc. 2nd Int. Conf. Image, Vis. Comput. (ICIVC)*, Jun. 2017, pp. 928–932.
[60] M. Kanno, "Canonical analysis of commodity flows and socio-economic structure in major US metropolitan areas," *Geograph. Rev. Jpn.*, vol. 49, no. 4, pp. 197–216, 1976.
[61] R. A. Murdie, "The factorial ecology of metropolitan toronto: 1951 and 1961," Dept. Geography. Res. Papers, Univ. Chicago, IL, USA, Tech. Rep. 116, 1969, p. 212.
[62] C.-G. Janson, "A preliminary report on Swedish urban spatial structure," *Econ. Geography.*, vol. 47, p. 249, Jun. 1971.
[63] W. Christaller. *Central Places in Southern Germany*. Englewood Cliffs, NJ, USA: Prentice-Hall,1966.

PEIQUN LIN received the B.S. degree from the School of Transportation and Communication Engineering, South China University of Technology, in 2003, and the Ph.D. degree from the School of Automation Science and Engineering, South China University of Technology, in 2008. He is currently a Professor with the South China University of Technology, Guangzhou, China. He has coauthored more than 40 journal publications and more than 15 peer-reviewed conference papers. He holds 15 Chinese patents and has a few patents pending in China. His research interests include connected vehicle networks, transportation system simulation, computer vision, and transportation big data analytics.

YITAO HE was born in Zhuhai, Guangdong, in 1997. He received the B.E. degree in transportation engineering from the South China University of Technology, in 2019, and the dual degrees in finance from the South China University of Technology, in 2019, where he is currently pursuing the M.S. degree. From 2016 to 2019, he participated in various programs, including Multi-objective Tracking Technology for Public Travel and Application and Prospect of Electric Scooter. His research interests include traffic information engineering and big data analysis. He received the third price in the China Internet + transportation Innovation and Entrepreneurship Competition.

MINGYANG PEI received the B.S. degree in transportation engineering from the South China University of Technology, in 2015, and the master's degree in 2017. She is currently pursuing the Ph.D. degree in transportation engineering with the South China University of Technology under the supervision of P. Lin. She has also been a visiting Ph.D. candidate with the University of South Florida for a two-year program, under the supervision of X. Li, since 2018. Her research interests include transportation modeling and computer vision and the transportation of big data analytics.